GLIA

WILEY

Check for updates

RESEARCH ARTICLE

A reporter cell system for the triggering receptor expressed on myeloid cells 2 reveals differential effects of disease-associated variants on receptor signaling and activation by antibodies against the stalk region

Melanie Ibach[1] | Mona Mathews[2] | Bettina Linnartz-Gerlach[3] | Sandra Theil[1] | Sathish Kumar[1] | Regina Feederle[4,5] | Oliver Brüstle[2,6] | Harald Neumann[3] | Jochen Walter[1]

[1]Department of Neurology, University of Bonn, Bonn, Germany

[2]Life and Brain GmbH, Bonn, Germany

[3]Neural Regeneration, Institute of Reconstructive Neurobiology, University of Bonn Medical Faculty & University Hospital Bonn, Bonn, Germany

[4]Institute for Diabetes and Obesity, Monoclonal Antibody Core Facility, Helmholtz Zentrum München, German Research Center for Environmental Health, Neuherberg, Germany

[5]Core Facility Monoclonal Antibodies, German Center for Neurodegenerative Diseases (DZNE), Munich, Germany

[6]Institute of Reconstructive Neurobiology, University of Bonn Medical Faculty & University Hospital Bonn, Bonn, Germany

Correspondence
Jochen Walter, Department of Neurology, University of Bonn, Bonn, Germany.
Email: jochen.walter@ukbonn.de

Abstract

The triggering receptor expressed on myeloid cells 2 (TREM2) is an immune receptor expressed on myeloid-derived cell types. The extracellular immunoglobulin-like domain of TREM2 binds anionic ligands including Apolipoprotein E and Amyloid-β. The transmembrane domain interacts with its adaptor protein DAP12/TYROBP that is responsible for propagation of downstream signaling upon ligand interaction. Several sequence variants of TREM2 have been linked to different neurodegenerative diseases including Alzheimer's disease. Here, we generated HEK 293 Flp-In cell lines stably expressing human TREM2 and DAP12 using a bicistronic construct with a T2A linker sequence allowing initial expression of both proteins in stoichiometric amounts. Cell biological and biochemical analyses revealed transport of TREM2 to the cell surface, and canonical sequential proteolytic processing and shedding of TREM2 (sTREM2). The functionality of this cell system was demonstrated by detection of phosphorylated spleen tyrosine kinase (SYK) upon stimulation of TREM2 with the anionic membrane lipid phosphatidylserine or anti-TREM2 antibodies. Using this cell model, we demonstrated impaired signaling of disease associated TREM2 variants. We also identified a monoclonal antibody against the stalk region of TREM2 with agonistic activity. Activation of TREM2-DAP12 signaling with the monoclonal antibody and the partial loss of function of disease associated variants were recapitulated in induced pluripotent stem cell derived microglia. Thus, this reporter cell model

represents a suitable experimental system to investigate signaling of TREM2 variants, and for the identification of ligands and compounds that modulate TREM2-DAP12 signaling.

1 | INTRODUCTION

The triggering receptor expressed on myeloid cells 2 (TREM2) belongs to the immunoglobulin superfamily of cell surface receptors encoded by a gene cluster located on chromosome 6p21 (Allcock, Barrow, Forbes, Beck, & Trowsdale, 2003; Klesney-Tait, Turnbull, & Colonna, 2006). It is expressed on myeloid-derived cell types including dendritic cells, osteoclasts, tissue macrophages, and microglia (Colonna, 2003b; Colonna & Wang, 2016; Paloneva et al., 2003). The receptor represents a type I membrane protein with an extracellular region containing a single immunoglobulin-like domain which binds anionic lipids and lipoproteins including Apolipoprotein E (Atagi et al., 2015; Y. Wang et al., 2015; Yeh, Wang, Tom, Gonzalez, & Sheng, 2016). Amyloid-β has also been identified as a TREM2 ligand (Zhao et al., 2018; Zhong et al., 2018). The short cytoplasmic domain of TREM2 has no known signaling function. However, TREM2 associates with its adaptor protein DAP12 (DNAX activation protein of 12 kDa, TYROBP) via interactions of charged residues within the transmembrane domains of both proteins (Paloneva et al., 2002). The cytoplasmic domain of DAP12 contains a characteristic immunoreceptor tyrosine-based activation motif, which is phosphorylated upon ligand-binding to TREM2, and thereby regulates several intracellular signaling pathways that control cell proliferation and differentiation, survival, phagocytosis, and cytoskeletal remodeling as well as calcium mobilization and cytokine production (Colonna, 2003a; Jay, von Saucken, & Landreth, 2017; Walter, 2016).

TREM2 is mainly found intracellularly either within the trans-Golgi network or in exocytic vesicles (Prada, Ongania, Buonsanti, Panina-Bordignon, & Meldolesi, 2006). TREM2 can undergo proteolytic cleavage between amino acids H157 and S158 by members of the a disintegrin and metalloproteinase (ADAM) family (Feuerbach et al., 2017; Schlepckow et al., 2017; Thornton et al., 2017). This cleavage results in the release of a soluble TREM2 ectodomain (sTREM2) into extracellular fluids, and generation of a membrane-tethered C-terminal fragment (CTF) (Kleinberger et al., 2014; Wunderlich et al., 2013). The TREM2 CTF represents a substrate for intramembrane proteolysis by γ-secretase (Wunderlich et al., 2013), that is also expressed in microglia (Farfara et al., 2011; Kemmerling et al., 2017; Nadler et al., 2008; Walter, Kemmerling, Wunderlich, & Glebov, 2017). Recently, it has been shown that sTREM2 can promote microglial survival and lead to the production of inflammatory cytokines, suggesting an important role in the immune response of microglial cells in neurodegenerative diseases (Zhong et al., 2017). Long and short-term expression of sTREM2 could also reduce Aβ plaque burden in a mouse model of Alzheimer's disease (AD; Zhong et al., 2019). Additionally, TREM2 has been shown to be highly abundant on microglia-associated plaques in AD brains (Frank et al., 2008) and showed involvement in synapse elimination and regulation of synaptic refinement (Filipello et al., 2018; Jay et al., 2019).

Interestingly, several mutations in TREM2 have been linked to different neurodegenerative diseases. Loss of function mutations were first identified in Nasu–Hakola disease (NHD, also known as polycystic lipomembranous osteodysplasia with sclerosing leukoencephalopathy; Hakola, Järvi, & Sourander, 2009; Nasu, Tsukahara, & Terayama, 1973), characterized by bone cysts, fractures, and dementia associated with axonal degeneration, increased microglial activation and neuroinflammation (Kaneko, Sano, Nakayama, & Amano, 2010; Satoh et al., 2011). Similar neurological symptoms have been discovered in frontotemporal dementias (FTDs; Humphrey, Xing, & Titus, 2015). The TREM2 variant T66M has been shown to be a cause for NHD in homozygous carriers (Le Ber et al., 2014). TREM2 T66M shows a decreased cell surface expression, caused by impaired protein folding and decreased transport from the endoplasmic reticulum (ER) to the plasma membrane (Kleinberger et al., 2014; Kober et al., 2016). Accordingly, the T66M variant showed significantly lower secretion of sTREM2 (Kleinberger et al., 2014).

Some rare TREM2 variants are also associated with an increased risk of developing AD. Here, the R47H variant increases the risk for AD 2–3 fold, comparable to the effect of the apolipoprotein ε4 allele (Guerreiro et al., 2013; Jonsson et al., 2013). The R47H substitution is located in the ligand-binding site within the Ig-like domain and decreases the interaction with anionic lipids (Kober et al., 2016). Recently, the R47H variant was also shown to impair functions of sTREM2 in microglial survival and inflammatory responses (Zhong et al., 2017). A novel TREM2 G145W variant segregating with early onset dementia in a family appears to cause changes in the protein conformation, thus affecting the function and signaling of TREM2 (Karsak et al., 2020).

Here, we describe a robust cellular model system to study characteristics of TREM2 common and rare variants in subcellular transport, expression at the cell surface, and TREM2-DAP12 receptor complex mediated signaling. Application of this system revealed differential effects of the distinct TREM2 variants on cell surface exposure, receptor proximal signaling, and cellular response. Thus, this system could facilitate the investigation of molecular mechanisms underlying the effects of disease associated mutations of the TREM2-DAP12 complex, and the identification of natural ligands and compounds that modulate TREM2-DAP12 signaling. An agonistic antibody against the stalk region of TREM2 showed specific induction of TREM2-DAP12 signaling, which might be further explored in future therapeutic approaches.

2 | MATERIALS AND METHODS

Cell culture media and corresponding supplements were ordered from *ThermoFisher Scientific, Austin, TX*. Fetal calf serum (FCS) was purchased from *PAN Biotech, Aidenbach, Germany*, dimethylsulfoxid (DMSO) was purchased from *Carl Roth GmbH & Co. KG, Karlsruhe, Germany*. Consumables were purchased from *Sarstedt AG & Co, Nürnbrecht, Germany*. Other substances, as not otherwise stated, were ordered at *Sigma-Aldrich Chemie GmbH, Munich, Germany; Carl Roth GmbH & Co. KG* or *ThermoFisher Scientific*.

2.1 | Primary and secondary antibodies

Following primary antibodies were obtained from the indicated providers: goat polyclonal anti-hTREM2 (AF1828, R&D Systems), rat monoclonal anti-mTREM2 (MAB1729, R&D Systems), rabbit monoclonal anti-DAP12 (ab124834, abcam), rabbit polyclonal anti-Calnexin (H-70, Santa Cruz biotechnology), rabbit polyclonal anti-TGN46 (T7576, Sigma Aldrich), mouse monoclonal anti-SYK (4D10, Cell Signaling), rabbit monoclonal anti-pSYK (Tyr525/526, C87C1, Cell Signaling). The mouse monoclonal anti-hTREM2 4B2A3 was generated by immunization of mice with the human TREM2 ectodomain from amino acids 19–174. Hybridoma cells were generated and binding to TREM2 characterized by enzyme-linked immunosorbent assay (ELISA). For cellular experiments, the antibody was affinity purified from the conditioned medium of hybridoma cells. Rat monoclonal antibody 9D11 against the C-terminus of human TREM2 was described previously (Schlepckow et al., 2017). For generation of anti-hTREM2 antibody T2EC 17C9 (IgG2b/k), Lou/c rats were immunized with a mixture of 60 µg purified his-tagged human TREM2 ectodomain, 5 nmol CpG (TIB MOLBIOL), and an equal volume of incomplete Freund's adjuvant. After a 6 weeks interval, a final boost was given 3 days before fusion of spleen cells with P3X63Ag8.653 myeloma cells using standard procedures. Hybridoma supernatants were screened in a solid-phase ELISA for binding to TREM2 protein. Positive supernatants were further assayed for their potential in immunoblotting and immunofluorescence. Hybridoma cells from selected supernatants were subcloned at least twice by limiting dilution to obtain stable monoclonal cell lines.

As secondary antibodies, HRP-conjugated goat anti-rat (Rockland), rabbit anti-goat, goat anti-rabbit and rabbit anti-mouse (Sigma Aldrich) and Alexa Fluor 488-conjugated Anti-mouse, Alexa Fluor 488-conjugated Anti-goat, Alexa Fluor 546-conjugated Anti-rabbit and Alexa Fluor 546-conjugated Anti-mouse (Thermo Fisher Scientific) were used.

2.2 | Cell culture

The human embryonic kidney cell line HEK 293 was cultured in DMEM medium supplemented with 10% heat-inactivated FCS and 1% Penicillin/Streptomycin at 37°C in a 5% CO_2 atmosphere. Medium for HEK 293 Flp-In cells was supplemented with 100 µg/ml Zeocin. Plasmid transfected HEK 293 Flp-In cells were cultured in cell culture medium supplemented with 100 µg/ml Hygromycin B.

The TREM2 homozygous knockout (TREM2 KO; Bioni 010 C17), TREM2 homozygous R47H variant (TREM2 R47H; Bioni 010 C-7) and TREM2 homozygous T66M variant (TREM2 T66M; Bioni 010 C-8) were generated isogenically from the TREM2 wild type parental line (TREM2 wt; Bioni 010 C). All lines were kindly provided by Janssen Pharmaceutica and deposited at EBiSC, European Bank for induced pluripotent Stem Cells (https://cells.ebisc.org). All induced pluripotent stem cell (iPSC)-based culture and differentiations were carried out by LIFE & BRAIN GmbH. The cells were cultured in 6-well plates coated with Geltrex (18 µg/ml in DMEM/F-12, Life Technologies) in StemMACS™ iPS-Brew XF medium (STEMCELL Technologies) and passaged with 0.5 mM EDTA in PBS (Sigma). Human iPSC-derived microglia (iPSdMiG) were custom-produced from the above four TREM2 genotypes by LIFE & BRAIN GmbH according to a previous established proprietary protocol. To start the differentiation into iPSdMiG, iPSCs were cultured until 70–80% confluency and detached as intact colonies by incubating with freshly prepared collagenase IV (1 mg/ml in DMEM/F-12, Gibco) for 30 min at 37°C. Subsequently, the detached colonies were transferred to non-tissue culture dishes for embryoid body (EB) generation in suspension culture and subsequently further differentiation into iPSdMiG. The iPSdMiG were produced from 4 to 6 weeks of differentiation and were harvested from the supernatant during the following 7-week peak production phase. Harvested iPSdMiG were plated onto poly-L-lysine (PLL)-coated culture dishes and experiments were carried out 24 hr after plating.

2.3 | Plasmid transfections

For transfection of plasmids, cells were seeded in 6 cm cell culture dishes. The next day, an appropriate amount of DNA plasmid was mixed in 200 µl Opti-MEM Reduced Serum medium, as DNA-Lipofectamine 2000 complexes must be made in serum-free conditions. Lipofectamine 2000 was diluted in Opti-MEM 1:20 in a total volume of 200 µl for each transfection. Lipofectamine and plasmid preparations were mixed and incubated for 15 min at room temperature (RT). Lipofectamine-plasmid complexes were dropwise added to 6 cm dishes, and cells incubated under cell culture conditions. For stable transfections in HEK 293 Flp-In cells, a co-transfection of 7.2 µg pOG44 coding for Flp recombinase and 0.8 µg of respective constructs in a pcDNA5/FRT vector (Invitrogen) was performed. Also, 24 hrs post transfection medium was replaced with culturing medium supplemented with 100 µg/ml Hygromycin B for selection of cells expressing the respective gene of interest. For generation of TREM2-Fc fusion constructs, pFUSE-hIgG1-Fc1 and pFUSE-hIgG1-Fc2 (including IL2 signal sequence for secretion of fusion proteins) were used (Invivogen).

2.4 | Biotinylation of cell surface proteins

Cells were cultured on PLL coated 6 cm cell culture dishes to a confluency of 80–90%. For biotinylation of cell surface proteins, cells were kept on ice and washed twice with ice-cold PBS. Subsequently, cells were incubated with 0.5 mg/ml Sulfo-NHS-biotin in PBS under constant gentle shaking. The biotin solution was removed and cells were washed three times with 20 mM glycine in PBS, incubating the last wash step for 15 min. Cells were washed again with ice-cold PBS prior to cell lysis for 15 min with 900 μl STEN lysis buffer (150 mM NaCl, 50 mM Tris, 2 mM EDTA, 1% NP-40, 1% Triton X-100 in dH_2O, pH 7.4). Insoluble cell fractions were removed by centrifugation for 10 min, 12.000g and 4°C. In parallel, streptavidin-sepharose was washed three times with PBS, followed by one wash step with STEN buffer (150 mM NaCl, 50 mM Tris, 2 mM EDTA, 0.2% NP-40 in dH_2O, pH 7.6). Beads were used as 50% in STEN buffer. Fifty micro liter of washed streptavidin-sepharose was added to cell lysates and incubated over night at 4°C on an overhead shaker. Streptavidin-sepharose was washed four times for 10 min with STEN buffer and centrifuged for 3 min at 600g and 4°C. Samples were supplemented with 20 μl 2× SDS loading buffer and boiled for 5 min at 95°C. Further, samples were analyzed by SDS-PAGE and western blot analysis.

2.5 | AlphaLISA technology

Detection of phospho-SYK in cell lysates after stimulation of TREM2 was performed according to manufacturer's instructions (AlphaLISA® *Sure-Fire® Ultra*™, Perkin Elmer). Briefly, cells were treated with TREM2 ligands for indicated time points. Subsequently, cells were lysed with 1× Lysis Buffer for 10 min. Ten micro liter of cell lysates were transferred into a 384-well Optiplate and incubated with 5 μl Acceptor Mix for 1 hr in the dark. Fiv micro liter Donor Mix was added and the mixture was incubated for another 1 hr in the dark. The Optiplate was measured using an Envision® reader with standard AlphaLISA settings.

2.6 | Immunocytochemistry

Cells were plated on PLL coated coverslips and subsequently fixed with 4% pre-warmed PFA in PBS for 20 min. Cells were washed three times with PBS and incubated with solution I (0.25% Triton X-100) for 2 min at RT for permeabilization of the cellular membrane. Cells were blocked for 1 hr with solution III (2.5% BSA in 0.125% Triton X-100). Incubation with primary antibodies was performed in solution IV (0.125% BSA in 0.125% Triton X-100) for 1 hr at RT in a humidified chamber. Afterward, cells were washed three times with solution II (0.125% Triton X-100) followed by 1 h incubation at RT with DAPI and the appropriate secondary antibody conjugated with fluorophores. Cells were rinsed three times with solution II followed by two wash steps with PBS, and shortly dipped in dH_2O before mounting on microscopic slides using Immu-Mount (ThermoFisher Scientific). Images were obtained using a Leica SP8 Lightning confocal microscope and were further analyzed with ImageJ (NIH).

For selective staining of cell surface proteins, cells were seeded on PLL coated coverslips in 24-well plates. At the desired confluency, cells were washed once with warm DMEM medium. Plates were placed on ice and cells were incubated for 1 hr with the primary antibody in DMEM. After gentle washing with ice-cold DMEM for three times, cells were incubated for 1 hr with the corresponding secondary antibody conjugated with fluorophores. Prior to fixation with 4% PFA, another wash step with ice-cold DMEM was performed. Cells were washed three times with PBS and cell membranes were permeabilized with 0.25% Triton X-100 in PBS for 2 min. Nuclei were stained with DAPI and coverslips were washed three times with PBS and once with dH_2O. Eventually, cells were mounted on microscopic slides using Immu-Mount and images were obtained as described above.

2.7 | Protein precipitation with trichloroaceticacid

After collection of cell culture medium, the suspension was centrifuged at 600g for 10 min at 4°C. Supernatant was transferred into a fresh tube and sodiumdeoxycholat (NaDOC) was added to achieve a final concentration of 0.02%. The solution was inverted and incubated for 15 min at RT. trichloroaceticacid (TCA) was added to a final concentration of 10%, again, samples were inverted and incubated for 1 hr at RT for precipitation of proteins. Subsequently, the suspension was centrifuged at 16.000g and 4°C for 10 min. The supernatant was discarded and samples were centrifuged again. Remaining supernatant was removed and samples were resuspended in an appropriate volume of 50 mM Tris/1% SDS buffer and SDS sample buffer was added. Samples were boiled at 95°C for 5 min and separated using SDS-PAGE.

2.8 | Membrane preparation

For preparation of cellular membranes, cells in dishes were washed with ice-cold PBS, scraped in an appropriate volume of hypotonic buffer (10 mM Tris, 1 mM EDTA, 1 mM EGTA in dH_2O, pH 7.6) supplemented with 1× protease inhibitor cocktail and collected in tubes. Cells were incubated on ice for 10 min and subsequently lysed using a syringe with a 0.6 mm cannula, drawing 20 times. After centrifugation for 5 min at 1.300g and 4°C, the supernatant containing cell membrane and cytosol was transferred into a fresh tube and centrifuged for 1 hr at 16.000g and 4°C. The supernatant (cytosol) was removed and the remaining pellet was lysed in 1× STEN lysis buffer supplemented with 1× protease inhibitor cocktail. Cell membranes were incubated for another 20 min on ice. The lysate was further centrifuged for 10 min at 16.000g and 4°C and the resulting supernatant was used for immunobiochemical analysis.

2.9 | Protein deglycosylation

For deglycosylation, TCA precipitated conditioned media of stable TREM2 wt cells resuspended in 50 mM Tris were incubated with

PNGase F, Endo H, or Endo D (NEB). Preparation of samples was performed according to the manufacturer's instructions. Briefly, samples were denatured for 10 min at 100°C with corresponding buffers and mixed with the respective glycosidase. The reaction was incubated at 37°C for 1 hr and stopped by addition of SDS loading buffer. Samples were analyzed by SDS-PAGE and western blotting analysis.

2.10 | Statistical analysis

Data were analyzed using GraphPad Prism 6 (La Jolla, USA). All data were tested for normality and subsequently analyzed by one-way ANOVA followed by post hoc Tukey's multiple comparisons test or Student's t-test (unpaired, two-tailed). A p-value less than .05 was considered as statistically significant (*p <.05; **p <.01; ***p <.001). For statistical analysis, at least three independent experiments were analyzed.

3 | RESULTS

3.1 | Generation and characterization of a TREM2-DAP12 reporter cell system

In order to allow expression of TREM2 and its co-receptor DAP12 in stoichiometric amounts, a bicistronic construct encoding human TREM2 and DAP12 separated by a T2A peptide sequence was cloned into the Flp-In vector (Figure 1a), and used to transfect HEK 293 Flp-In cells with an endogenous Flp recombination target (FRT) site. A plasmid encoding the Flp recombinase was co-transfected. Stable single cell clones were selected and expression of TREM2 and DAP12 was analyzed by Western immunoblotting in purified cellular membrane fractions (Figure 1b). In parallel, we also included transiently transfected cells for comparison. TREM2 was detected as mainly immature protein of approximately 38 kDa in stably and transiently transfected cells. In addition, TREM2 CTFs migrating below 15 kDa were also observed upon transient and stable transfection, however, in different amounts. Comparison of stable and transient transfection also revealed differences in the relative amounts of DAP12 monomers (12 kDa), dimers (24 kDa), trimers (36 kDa), and higher assemblies.

TREM2 can undergo proteolytic cleavage by ADAM proteases, resulting in the secretion of its ectodomain (Kleinberger et al., 2014; Wunderlich et al., 2013). In supernatants, secreted soluble TREM2 (sTREM2) was detected as diffuse signals between 35 and 55 kDa rather than as distinct bands (Figure 1B), consistent with complex *N*-glycosylation within the TREM2 ectodomain (Kleinberger et al., 2014; Park et al., 2015). To test *N*-glycosylation of TREM2, secreted TREM2 from conditioned media was subjected to deglycosylation. Treatment with PNGase F resulted in the disappearance of the diffuse smear and formation of a distinct ~17 kDa band, representing deglycosylated TREM2 (Figure 1c). In contrast, the higher molecular weight smear was largely resistant against deglycosylation with Endo D and Endo H

(Figure 1c). Together these results indicate that sTREM2 from stably expressing cells mainly contains mature mannose-poor glycostructures. However, sTREM2 secreted from transiently transfected cells showed different migration in SDS gels than that from stably transfected samples (Figure 1b), indicating differences in the maturation of TREM2 by glycosylation.

In addition, specific labeling of cell surface proteins by biotinylation showed formation of high molecular weight forms for both, TREM2 and DAP12 in transiently transfected cells, further suggesting aberrant maturation and assembly upon transient over-expression of these proteins (Figure 1d). Biotinylated DAP12 is mainly migrating at ~24 kDa, indicating formation of characteristic stable dimers that are transported to the cell surface (Figure 1d). A ~38 kDa form of TREM2, likely representing immature TREM2, was also biotin-labeled in transiently transfected cells, indicating aberrant transport of immature TREM2 to the cell surface. Indeed, it has been shown that high overexpression of proteins could saturate retention and quality control systems in the ER and thus induce export and secretion of misfolded or immature proteins (Barlowe & Helenius, 2016; Hammond & Helenius, 1994). Thus, only cell lines stably co-expressing TREM2 and DAP12 were used for further experiments.

3.2 | Differential effects of TREM2 variants on subcellular transport, proteolytic processing, and secretion

Several TREM2 variants have been linked to neurodegenerative diseases. After the validation of the HEK 293 Flp-In cell system to stably co-express TREM2 and DAP12, we generated additional cell models for disease-associated variants of TREM2 together with DAP12. Beside the common (WT) TREM2 variant, we also used the R47H variant associated with an increased risk for AD (Guerreiro et al., 2013; Jonsson et al., 2013). In addition, we used the T66M variant associated with FTDs (Le Ber et al., 2014), and a novel G145W variant that has been shown to segregate with a familial form of dementia (Karsak et al., 2020). To investigate the secretion of the different TREM2 variants, levels of sTREM2 in cell supernatants, and those of full length TREM2 and TREM2 CTFs in cellular membranes were detected by Western immunoblotting (Figure 2a,b).

As compared to the common TREM2 variant, the AD associated R47H variant showed decreased levels of sTREM2 in cell supernatants. sTREM2 was hardly detectable in media of T66M expressing cells (Figure 2a,b). Similar effects of the R47H and T66M variant have been described previously in vitro and in vivo (Kleinberger et al., 2014; Song et al., 2018; Sudom et al., 2018), and were related to altered transport and maturation of these TREM2 variants. TREM2 CTFs were hardly detectable in cells expressing the TREM2 T66M variant, consistent with efficient retention of TREM2 T66M in the ER, thereby preventing proteolytic processing by ADAM proteases in post ER compartments. In addition, a higher band of ~70 kDa could be observed for this variant, possibly indicating accumulation of dimeric TREM2 T66M.
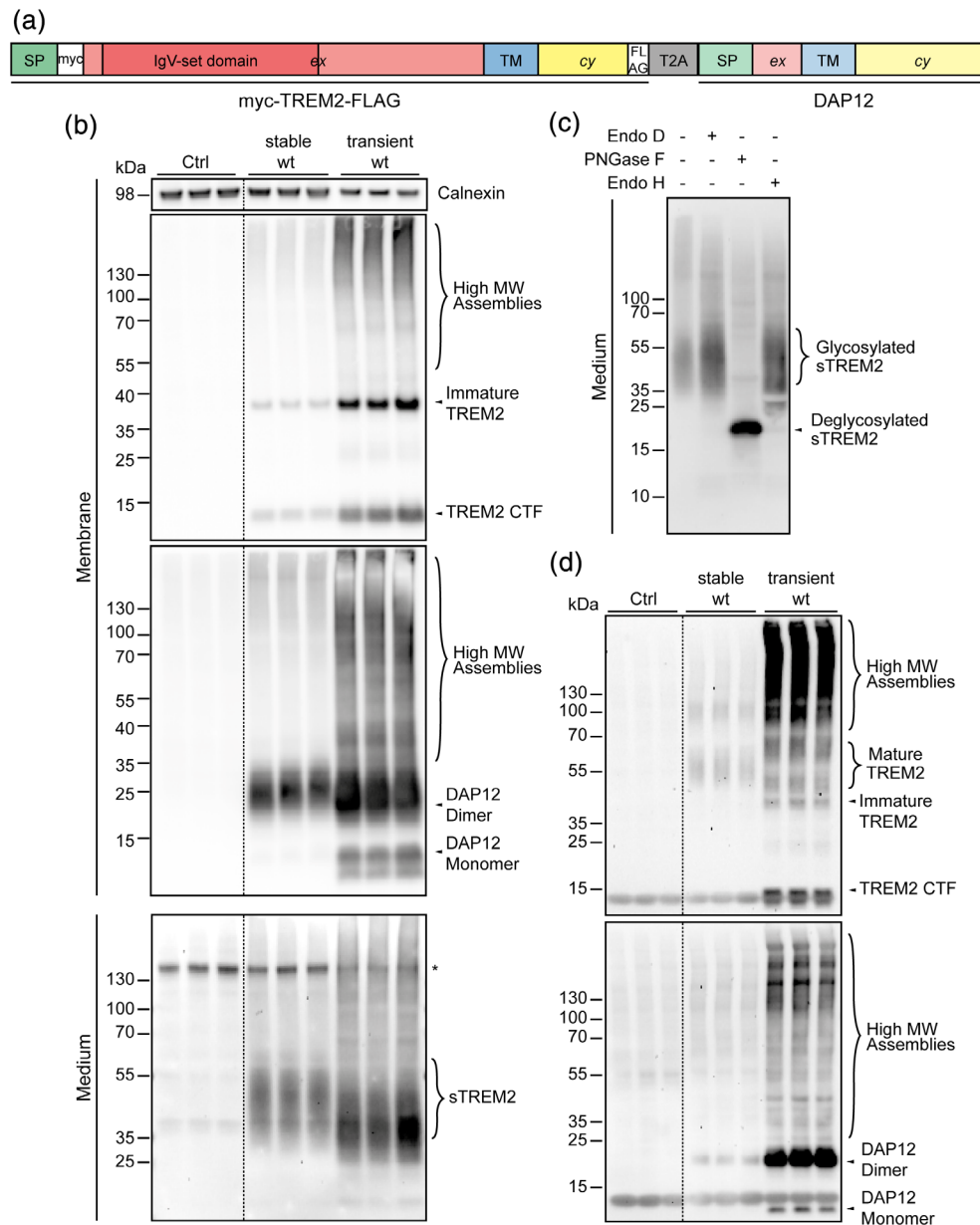
FIGURE 1 Expression and maturation of TREM2 and DAP12 in stably and transiently transfected cells. (a) Illustration of the bicistronic construct of TREM2 and DAP12, including a myc-tag after the signal peptide and a FLAG-tag behind the cytoplasmic region of TREM2. A T2A peptide separates TREM2 and DAP12 allowing equal initial translation of both proteins from one mRNA. SP, signal peptide; myc, myc-tag; *ex*, extracellular domain; TM, transmembrane domain; *cy*, cytoplasmic domain; FLAG, FLAG-tag. (b) Analysis of membrane proteins. Non-transfected HEK 293 Flp-In cells (Ctrl) were used as control. Transient transfection was performed and cells were incubated overnight. Cell culture medium of transiently and stably transfected cells was replaced with serum-free medium for secretion of sTREM2 for 6 hrs. Media were collected and precipitated using TCA. Membrane fractions were isolated and both were analyzed via western blotting. Anti-TREM2 9D11 antibody was used for detection of C-terminal TREM2. Anti-TREM2 AF1828 was used to detect sTREM2 in conditioned media. "*" Represents an unspecific signal also detected in untransfected cells. Anti-DAP12 ab124834 was used for detection of DAP12. Calnexin served as a loading control. (c) Digestion of TCA precipitated conditioned medium of TREM2 wt expressing cells. Samples were incubated with respective glycosidases at 37°C for 1 hr and subsequently analyzed by western blotting. (d) Cell surface expression of TREM2 and DAP12 after biotinylation. Western blot analysis of biotinylated cell surface proteins with Sulfo-NHS-biotin and Streptavidin-sepharose precipitation. Anti-TREM2 AF1828 was used for detection of mature TREM2 at the cell surface [Color figure can be viewed at wileyonlinelibrary.com]

Further, biotinylation and immunocytochemical detection of surface TREM2 revealed intracellular accumulation of TREM2 T66M and strongly decreased expression at the cell surface (Figures 2c and 3b, respectively).

Interestingly, shedding of the novel TREM2 G145W mutant was significantly decreased. This mutation was shown to cause changes in the protein conformation due to the glycine to tryptophan substitution in the stalk region connecting the Ig-like and transmembrane
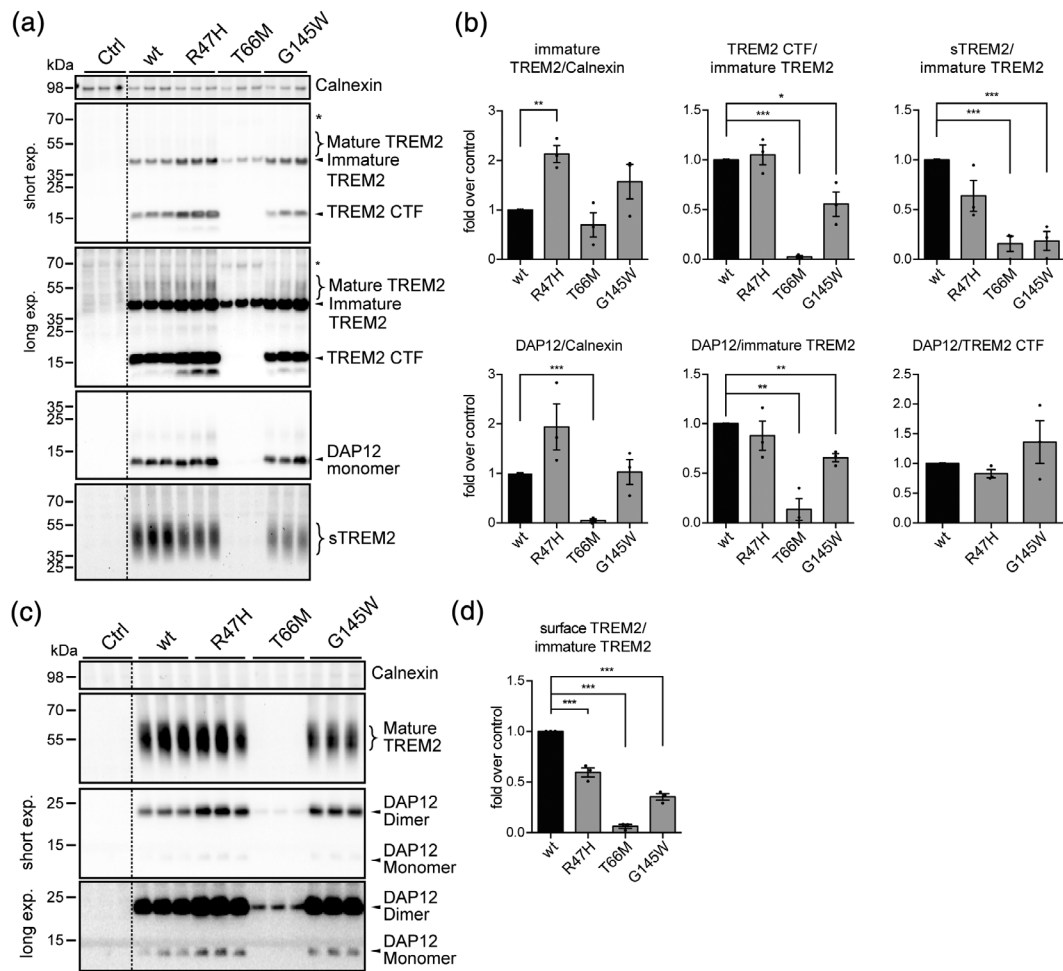
FIGURE 2 Comparative characterization of the common and disease associated TREM2 variants. (a) Monoclonal cell lines stably expressing TREM2 wt, R47H, T66M, and G145W were incubated with serum-free medium for 6 hrs for secretion of sTREM2. Media were collected and precipitated using TCA, membranes were isolated and both were analyzed via western blotting. Anti-TREM2 9D11 antibody was used for detection of C-terminal TREM2. Anti-DAP12 ab124834 was used for detection of DAP12. Anti-TREM2 17C9 antibody was used to detect sTREM2 in conditioned media. Calnexin served as a loading control for membrane fractions. "*" indictaes accumulation of TREM2 in T66M variant expressing cells. (b) Quantification of western blot analysis as shown in a. Data represent the mean ± *SEM* of three independent experiments with triplicate samples each. Student's *t*-test (unpaired, two-tailed), *p <.05; **p <.01; ***p <.001. (c) Cell surface expression of TREM2 and DAP12 after biotinylation. Western blot analysis of biotinylated cell surface proteins using Sulfo-NHS-biotin and Streptavidin-sepharose precipitation. Mature TREM2 was detected with 17C9 antibody. Calnexin served as a negative control for plasma membrane specific fractions. (d) Quantification of western blot analysis as shown in C. Data represent the mean ± *SEM* of three independent experiments with triplicate samples each. Student's *t*-test (unpaired, two-tailed), ***p <.001

domain of TREM2 (Karsak et al., 2020), that might also interfere with cell surface transport and efficient cleavage by ADAM proteases. As observed before (see Figure 1), biotin-labeled DAP12 was detected predoniantly as a specific band of ~23 kDa, which represents SDS-resistant DAP12 dimers (Figure 2c).

It has been reported that some disease-associated mutations alter the intracellular trafficking and thus the localization of TREM2 (Kleinberger et al., 2014; Park et al., 2015; Zhao et al., 2017). Here, immunocytochemistry revealed that all TREM2 variants, beside the T66M variant, localized mainly to the plasma membrane (Figures 3 and 4), where they co-localized with DAP12 (Figure 3a). Only minor fractions of TREM2 WT, R47H, and G145W co-localized with marker proteins for the ER (Calnexin) and the Golgi compartment (Giantin or TGN46, Figure 4). In contrast, the T66M variant showed strong co-localization with Calnexin (Figure 4a), consistent with previous results on efficient cellular retention of TREM2 T66M (Kleinberger et al., 2014; Park et al., 2015; Zhao et al., 2017).

Taken together, this reporter cell system revealed differential effects of distinct TREM2 variants on the subcellular localization and proteolytic processing, thereby partially confirming and extending previous results (Kober et al., 2016; Schlepckow et al., 2017; Thornton et al., 2017). In particular, all tested variants, including the recently identified TREM2 G145W variant showed lower expression at the cell surface when normalized to cellular levels of the full-length protein.
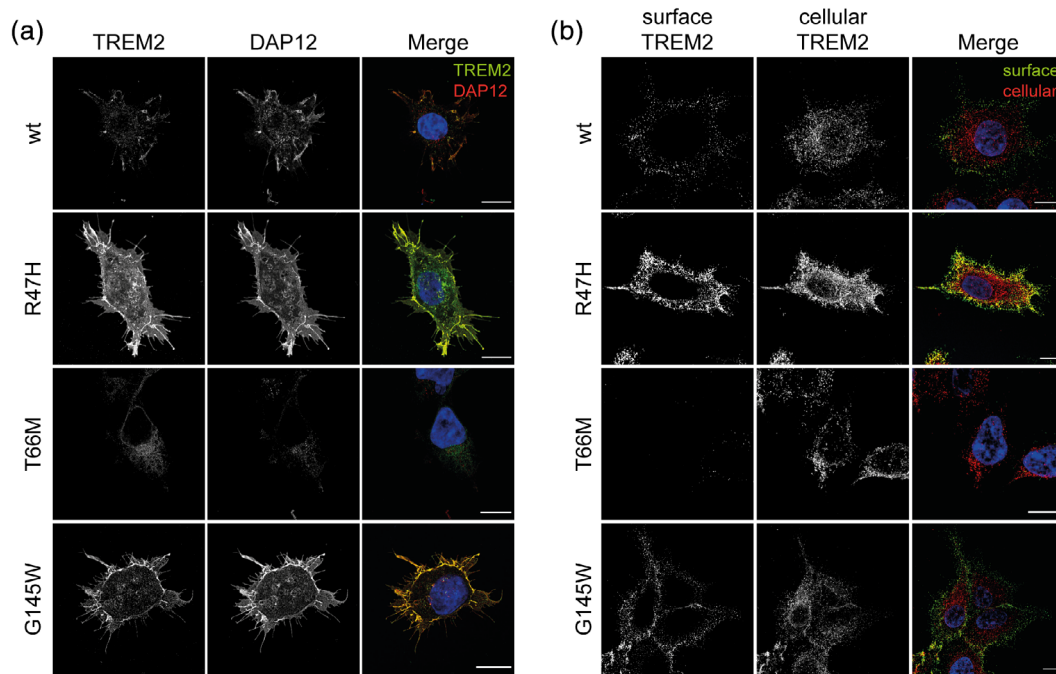
FIGURE 3 Immunocytochemical detection of TREM2 common and rare variants (a) Representative images of HEK 293 Flp-In myc-TREM2-FLAG_T2A_DAP12 cells for different variants of TREM2 with average intensity projection are shown. TREM2 (4B2A3 antibody) is shown in green and DAP12 in red. Nuclei were counterstained with DAPI. Scale bar = 10 μm. (b) Cell surface expression of TREM2. Cell surface TREM2 was stained with an ectodomain-specific antibody (4B2A3) in living cells without permeabilization (green). Subsequently, cells were fixed and cellular TREM2 was stained with ectodomain-specific antibody (AF1828, red). Nuclei were counterstained with DAPI. Scale bar = 10 μm [Color figure can be viewed at wileyonlinelibrary.com]
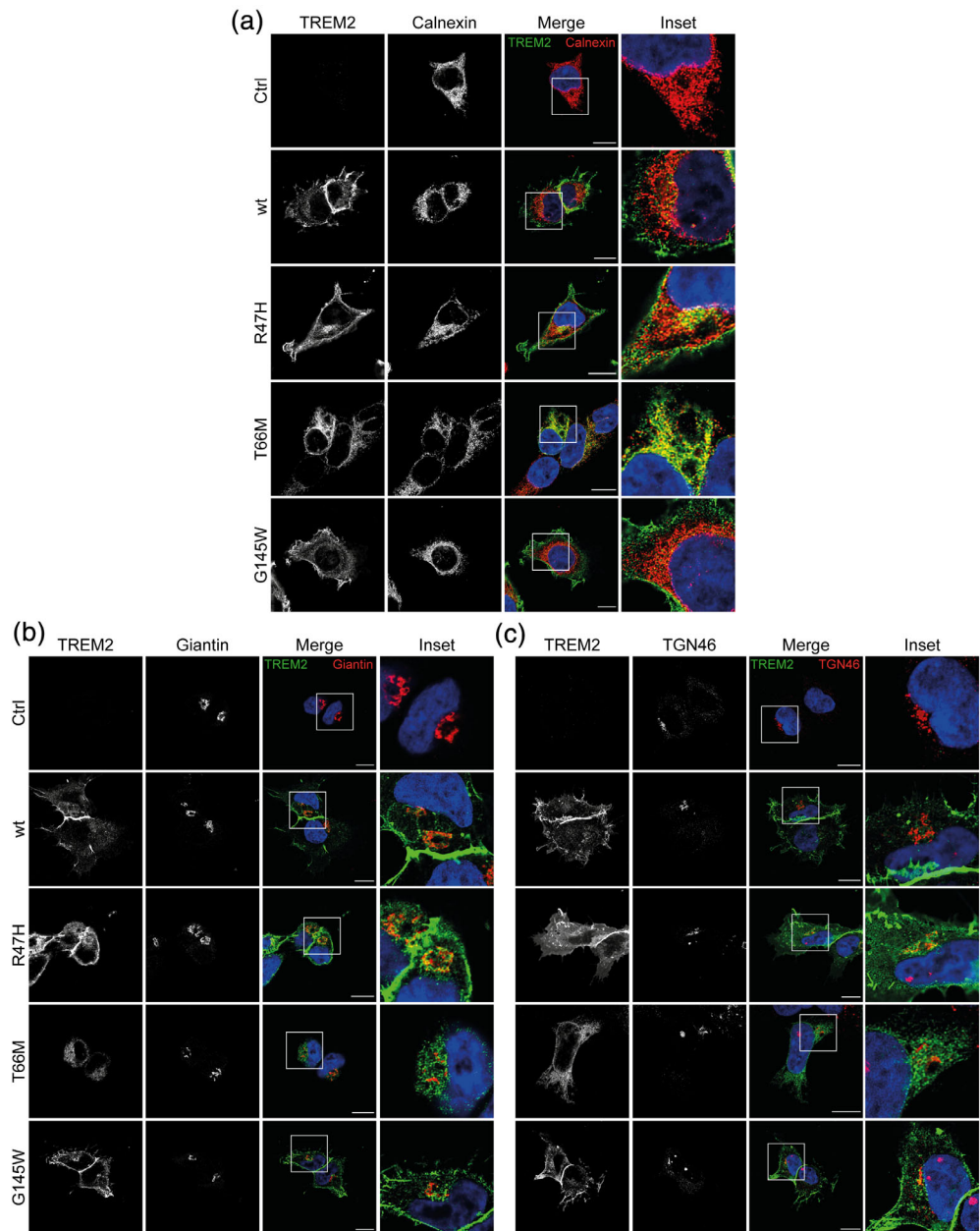
3.3 | A monoclonal anti-TREM2 antibody stimulates TREM2 signaling via cross-linking

Recently, agonistic activity of anti-TREM2 antibodies have been described (Price et al., 2020; Schlepckow et al., 2020; S. Wang et al., 2020). We developed a mouse monoclonal antibody against human TREM2 using the complete ectodomain of human TREM2 for immunization. To determine the epitopes of the respective antibody, constructs encoding fusion proteins of human Fc and different parts of the TREM2 ectodomain were generated (Figure 5a). Cells were transiently transfected and fusion proteins precipitated from the supernatant (Figure 5b). Western immunoblotting revealed that antibody 4B2A3 does not bind to the Ig-like domain, but selectively recognized an epitope within the stalk region of TREM2 (aa 131–148). The amino acid sequence of human TREM2 within the identified 4B2A3 epitope is similar, but not identical to murine TREM2 (Figure 5c), and western immunoblot analysis showed that the 4B2A3 antibody selectively detected human TREM2 (Figure 5c). Next, we investigated if and how the anti-TREM2 4B2A3 antibody could stimulate TREM2 signaling. Therefore, Fab, F(ab')$_2$, and Fc fragments of the 4B2A3 antibody were produced by proteolytic cleavage with papain and pepsin. Papain cleaves the whole IgG above the hinge region, creating two separate Fab fragments and one Fc fragment (Leslie, Melamed, & Cohen, 1971). In contrast, pepsin digests the Fc part of the antibody and thus produces F(ab')$_2$ fragments that are still connected by two disulfide bonds. Using Protein A resin, Fc fragments and undigested antibodies can be removed from the generated Fab and F(ab')$_2$ fragments of both reactions.

Notably, the antibody 4B2A3 specifically activated TREM2 signaling assessed by the detection of phosphorylated SYK (pSYK) using AlphaLISA technology (Figure 5d). Stimulation of SYK phosphorylation was also observed with the respective F(ab')$_2$ fragment, but not with the Fab or Fc fragments. The higher stimulation of SYK phosphorylation with F(ab')$_2$ as compared to the full antibody at equimolar concentrations could be due to increased access of F(ab')$_2$ to overexpressed TREM2, because of the smaller size compared to that of the full antibody. However, this needs to be further investigated. These data indicate that the antibody 4B2A3 or its F(ab')$_2$ fragment specifically stimulates TREM2-DAP12 signaling by induction of receptor dimerization.

To validate the obtained results in cells with endogenous TREM2 expression, we next used induced pluripotent stem cell-derived microglia (iPSdMiG). TREM2 wt iPSdMiG were incubated with anti-TREM2 4B2A3 antibody or respective antibody fragments F(ab)$_2$, Fab, and Fc (Figure 5d). The whole 4B2A3 antibody induced significantly increased levels of phosphorylated SYK. However, the stimulation of SYK phosphorylation was much lower as compared to that in the HEK 293 reporter cell line. This is likely due to much lower expression of endogenous TREM2 in microglia compared to strong overexpression in the HEK 293 reporter line as endogenous TREM2 could not be reliably detected by Western immunoblotting of iPSdMiG samples. Interestingly, the F(ab)$_2$ fragments of antibody 4B2A3, but not the corresponding Fab or Fc fragments led to increased pSYK levels. In contrast to the results with the HEK 293 reporter lines overexpressing TREM2 and DAP12, with iPSdMiG, the stimulation of SYK phosphorylation with the F(ab')$_2$

FIGURE 4 Subcellular localization of TREM2 common and rare variants. Shown are representative images with average intensity projection of stable HEK 293 Flp-In cells coexpressing different variants of TREM2 together with DAP12. TREM2 (4B2A3 antibody) is shown in green and Calnexin (Endoplasmic reticulum, a), Giantin (*cis*- and *medial*-Golgi network, b) or TGN46 (*trans*-Golgi network, c) in red. Nuclei were counterstained with DAPI. Scale bar = 10 μm [Color figure can be viewed at wileyonlinelibrary.com]

3.4 | Disease associated TREM2 variants impair cellular signaling

To characterize the effects of TREM2 variants on membrane-proximal signal transduction, anti-TREM2 antibody 4B2A3, and the anionic phospholipid phosphatidylserine (PtdS) were used for stimulation of

fragments tended to be slightly lower as compared to stimulation with the full antibody. The reason for this remains to be determined, but might be due to higher avidity of the full antibody as compared to that of the respective F(ab')$_2$ fragments thereby causing higher stimulation at lower expression levels of TREM2. Taken together, the combined results strongly indicate that the stimulation of SYK phosphorylation with anti TREM2 antibodies depends on dimerization or cross-linking of TREM2.

TREM2 common and rare variants. PtdS has been described as a ligand for TREM2 and to activate TREM2 signaling (Hsieh et al., 2009; Y. Wang et al., 2015). Control cells without expression of TREM2 and DAP12 did neither respond to the exposure with anti-TREM2-antibody nor to PtdS (Figure 6a), whereas TREM2 wt expressing cells showed an 11-fold increase in pSYK levels upon stimulation with the antibody against the stalk region of TREM2, and a four-fold increase with PtdS (Figure 6a). The TREM2 T66M variant was not stimulated by either of the treatments (Figure 6a), consistent with the lack of full-length TREM2 T66M at the cell surface (see Figures 2 and 3). Cells expressing variants R47H and G145W both showed a reduced induction of SYK phosphorylation compared to cells expressing the common (wt) variant of TREM2 with both stimuli, the anti-TREM2 antibody and PtdS (Figure 6a). As compared to TREM2 wt expressing cells, pSYK levels were reduced by 74 and 50%
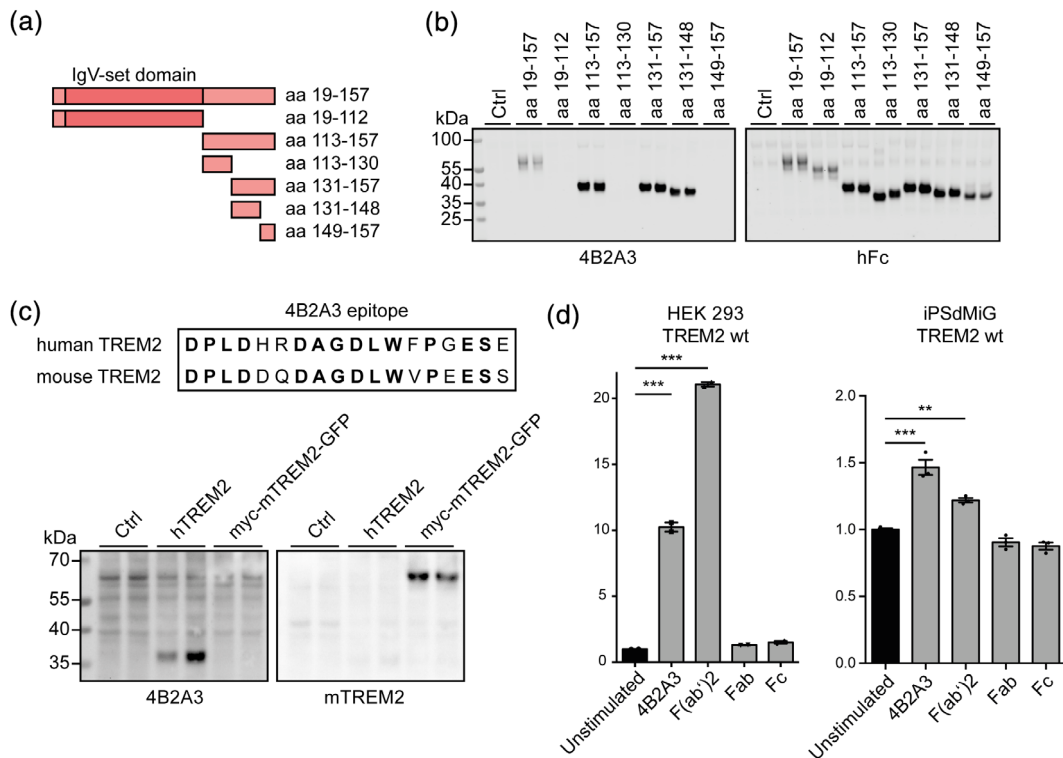
FIGURE 5 Anti-TREM2 4B2A3 antibody stimulates TREM2-DAP12 signaling via crosslinking. (a) Illustration of TREM2 fragments that were generated for investigation of TREM2 antibody binding. The sequences were C-terminally fused to human Fc and inserted into constructs with a signal sequence for secretion. (b) Cells were transfected with respective constructs shown in (a), and cell culture supernatants precipitated using TCA. Antibody 4B2A3 was used for detection of TREM2 fragments in western blot analysis. Anti-human Fc was used to detect all of the different fusion proteins. (c) Sequence of the 4B2A3 epitope in human and mouse TREM2. (d) Transient transfection of HEK 293 cells with constructs coding either human TREM2 (hTREM2) or mouse TREM2 (myc-mTREM2-GFP). Membrane fractions of transfected and non-transfected (Ctrl) cells were isolated and analyzed by western blot analysis. 4B2A3 antibody detects human TREM2 and mTREM2 antibody MAB1729 (R&D Systems) detects mouse TREM2. (e) HEK 293 Flp-In myc-TREM2-FLAG_T2A_DAP12 (left) and TREM2 wt iPSdMiG (right) were plated on PLL coated 96-well plates and treated for 5 min with 67 µM ectodomain-specific antibody or antibody fragments F(ab')$_2$, Fab, and Fc against TREM2 (4B2A3) or not treated as a control (unstimulated). Cells were lysed and lysates were analyzed for pSYK using AlphaLISA technologies. Data represent the mean ± *SD* of triplicate samples from one experiment. One-way ANOVA, Tukey's post hoc test for multiple comparison, *p <.05; **p <.01; ***p <.001 [Color figure can be viewed at wileyonlinelibrary.com]

for R47H and G145W expressing cells upon stimulation with PtdS, respectively. The R47H variant has been described to impair ligand binding of TREM2 (Atagi et al., 2015; Kober et al., 2016; Yeh et al., 2016), which could explain the decreased pSYK levels upon stimulation with PtdS. However, since antibody 4B2A3 binds to the stalk region of TREM2, it is unlikely that reduced activation of the R47H variant with this antibody is caused by decreased binding, but rather by the lower surface expression of this variant. Qualitatively very similar results were obtained when phosphorylated SYK and total SYK levels were detected by Western immunoblotting upon cell treatment with antibody 4B2A3 or PtdS (Figure 6b–g). However, with this detection method the magnitudes of stimulation were lower as compared to that obtained with the AlphaLISA technology, likely due to differences in the sensitivity and the detection range between both methods.

We also assessed the effect of the disease-associated variants R47H and T66M on the stimulation by antibody 4B2A3 in iPSdMiG (Figure 6h). As observed before, antibody 4B2A3 induced

phosphorylation of SYK in TREM2 wt expressing iPSdMiG. In contrast, levels of pSYK were not increased upon incubation with antibody 4B2A3 in TREM2 KO isogenic iPSdMiG. The stimulation of SYK phosphorylation was slightly lower in TREM2 R47H expressing iPSdMiG, and no stimulation was observed with isogenic TREM2 T66M iPSdMiG.

Together, these combined data further support a partial loss-of-function in the signaling capacity for the different disease associated variants of TREM2 as a common pathogenic effect.

4 | DISCUSSION

TREM2 mutations are linked to several neurodegenerative diseases, including NHD, FTD, and AD. Evidence suggests that most mutations result in a loss of function of TREM2, however, the exact molecular mechanisms underlying the effects of disease-associated mutations of TREM2 still remain unclear. Here, we established a robust cellular
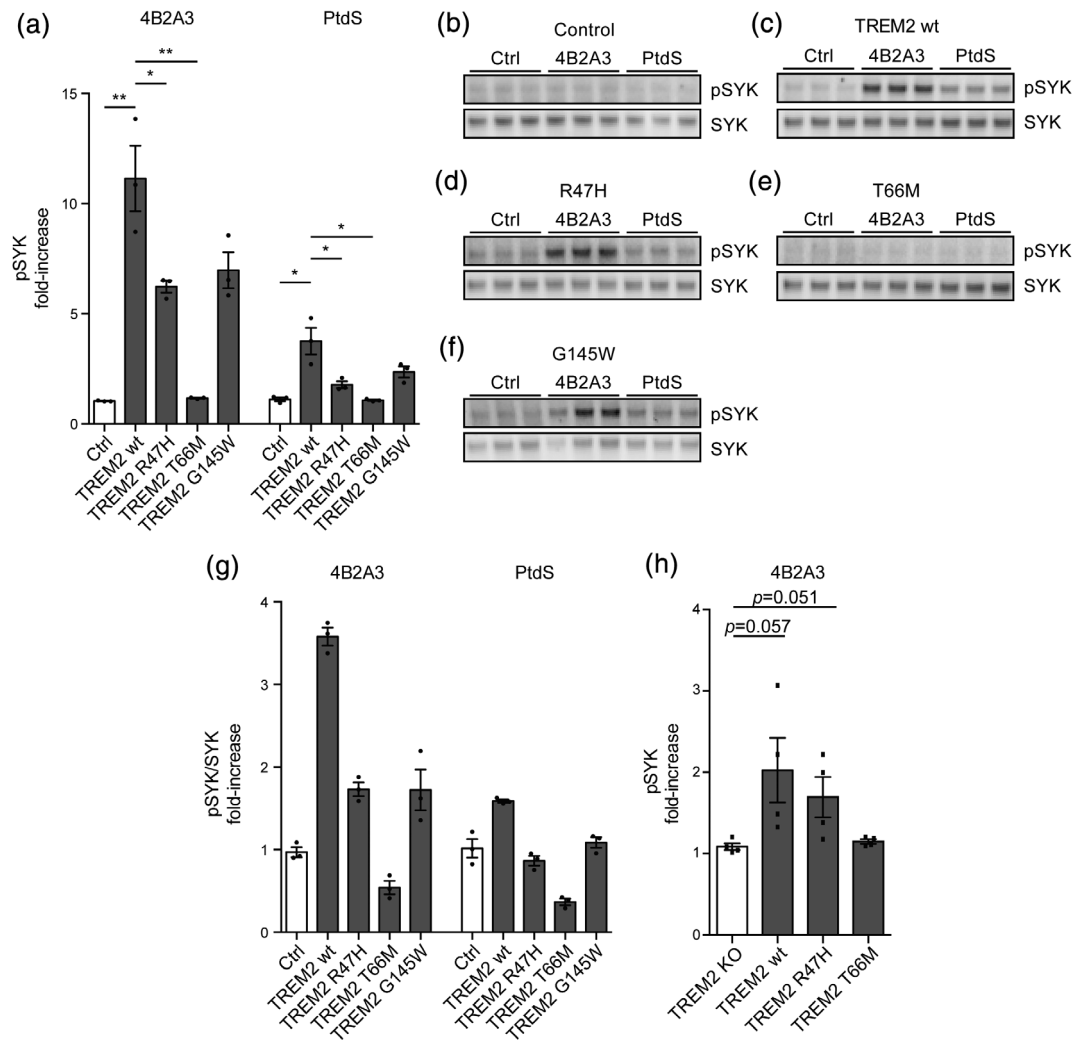
FIGURE 6 Differential activation of TREM2 variants by agonistic antibodies and phosphatidylserine. (a) HEK 293 Flp-In myc-TREM2-FLAG_T2A_DAP12 cells with TREM2 variants R47H, T66M, and G145W as well as control cells were plated on PLL coated 96-well plates and treated for 5 min with 10 μg/ml ectodomain-specific antibody against TREM2 (4B2A3), 50 μM Phosphatidylserine (PtdS), or not treated as a control (unstimulated). Cells were lysed and lysates were analyzed for pSYK using AlphaLISA technologies. Data represent the mean ± SEM of three independent experiments with triplicate samples each. Student's t-test (unpaired, tow-tailed), *p <.05; **p <.01. (b–f) Analysis of SYK and pSYK in cell lysates by Western immunoblotting. (g) Quantification of western blot analysis as shown in b–f. Data represent the mean ± SD from one experiment with biological triplicates. (h) TREM2 KO, wt, R47H and T66M expressing iPSdMiG were treated with 10 μg/ml 4B2A3 antibody for 5 min and lysates were analyzed for pSYK levels using AlphaLISA technologies. Data represent the mean ± SEM four independent experiments with triplicate samples each. Student's t-test (unpaired, two-tailed)

model system stably expressing TREM2 and its adaptor protein DAP12 in stoichiometric amounts. First, we observed that transient transfection of TREM2 and DAP12 resulted in aberrant maturation and transport of immature proteins to the cell surface (Figure 1). Due to these observations, a reporter cell system with stable co-expression of TREM2 and DAP12 was established that serves as a more reliable system to investigate TREM2-DAP12 signaling. This system allowed studying characteristics of TREM2 common and rare variants and TREM2-DAP12 receptor complex mediated signaling upon ligand binding. Application of this system revealed differential effects of the distinct TREM2 variants on subcellular localization and transport, cell surface exposure, receptor proximal downstream signaling, and cellular response.

As compared to the common TREM2 variants and other disease associated variants, the TREM2 T66M variants accumulated in the ER (Figure 2, marked with *), and was not detected at the cellular surface (Figures 2 and 3). It has already been reported that this mutation impairs N-glycosylation and trafficking to the plasma membrane (Kleinberger et al., 2014; Park et al., 2015). Additionally, TREM2 variants R47H and G145W also showed a lower, and the T66M variant an almost complete lack of cell surface expression in the reporter cell system.

The analysis of SYK phosphorylation upon stimulation of TREM2 suggests a partial loss of function for the disease-associated variants R47H, T66M, and G145W. PtdS is a phospholipid, integrated into the plasma membrane lipid bilayer. Under physiological conditions, PtdS is

restricted to the inner leaflet, however, during apoptosis PtdS is translocated to the external leaflet of the plasma membrane (Fadok et al., 1992). Recent studies have indicated that TREM2 binds PtdS and thus recognizes apoptotic or damaged cells (Hsieh et al., 2009; Y. Wang et al., 2015). Here, we also used PtdS to stimulate TREM2 signaling. PtdS efficiently stimulated the phosphorylation of SYK in cells expressing the common variant of TREM2, but all disease associated variants showed decreased activation of TREM2 signaling. Consistent with a complete lack of T66M on the cell surface, PtdS did not evoke phosphorylation of SYK, while the TREM2 R47H and G145W variants were still capable to promote SYK phosphorylation, albeit with lower potency. As shown in Figures 2 and 3, all tested rare disease-associated variants of TREM2 showed decreased cell surface levels. The lowered surface levels could potentially result from different mechanisms, including impaired transport (e.g., TREM2 T66M). Whether the decreased level of the R47H or the novel G145W variant is also due to altered subcellular transport and/or proteolytic processing remains to be determined. However, the lower levels of soluble TREM2 in conditioned media of these variants hint toward less efficient forward transport in the secretory pathway. The present data support and extent previous findings showing retention of some selected disease associated TREM2 variants in the ER and/or decreased maturation by glycosylation (Kleinberger et al., 2014; Park et al., 2015; Sirkis, Aparicio, & Schekman, 2017).

It has recently been shown that TREM2 CTF generated by proteolytic shedding of the ectodomain could be stabilized by its adaptor protein DAP12 (Zhong et al., 2015), and TREM2 CTF-DAP12 complexes could alter downstream signaling pathways (Glebov, Wunderlich, Karaca, & Walter, 2016; Yao et al., 2019). Thus, the changes in the relative levels of DAP12 and TREM2 CTF could also contribute to the observed impairment of TREM2 signaling. At least for the R47H variant, it has been shown that alterations in the amino acid sequence within the v-set Ig domain of TREM2 could interfere with ligand binding (Sudom et al., 2018; Y. Wang et al., 2015). Thus, in addition to the decreased cell surface expression, lower binding of ligands could also result in decreased signaling with the R47H variant. Since G145 is localized outside of the ligand-binding domain, it appears unlikely that the disease-associated substitution directly interferes with ligand interaction, albeit this possibility cannot be excluded.

Since the disease-associated variants studied here cause a partial or almost complete loss-of-function, activation of TREM2-DAP12 signaling could potentially represent a therapeutic approach to normalize regulation of microglial activity (Wes, Sayed, Bard, & Gan, 2016). Indeed, agonistic antibodies have been used to activate TREM2 signaling and even restore some cellular deficits observed in TREM2 R47H expressing cells (Cheng et al., 2018; Price et al., 2020; Schlepckow et al., 2020; S. Wang et al., 2020). The monoclonal anti TREM2 antibody 4B2A3 described here also had agonistic effects on TREM2-DAP12 signaling. This antibody does not bind to the ligand binding domain, however, it still stimulated TREM2 signaling through binding to the stalk region of TREM2 within amino acids 131–148 and activated TREM2 through receptor cross-linking. This could also be confirmed with iPSdMiG expressing endogenous TREM2, albeit at

much lower levels as compared to overexpressed TREM2 and DAP12 in the HEK 293 reporter line (Figure 5).

Notably, beside the T66M variant, stimulation by the 4B2A3 antibody was observed for the other disease-associated variants, even though to a lower extent as compared to the stimulation of the common TREM2 variant in both, HEK 293 reporter cells and iPSdMiG. Taken together, the reporter cell model described here represents a suitable system for studying cellular transport and metabolism of TREM2 and DAP12 and effects of disease associated TREM2 mutations. This system also allows the identification and characterization of compounds that modulate TREM2 activity for the development of future therapeutic strategies for AD and other neurodegenerative diseases. As the 4B2A3 anti-TREM2 specific antibody showed specific activation of TREM2 signaling in AD-associated risk variants, it might also represent a promising candidate for therapeutic approaches.

DATA AVAILABILITY STATEMENT

The data that support the findings of this study are available from the corresponding author upon reasonable request.

ORCID

Harald Neumann https://orcid.org/0000-0002-5071-5202
Jochen Walter https://orcid.org/0000-0002-4678-2912

REFERENCES

Allcock, R. J. N., Barrow, A. D., Forbes, S., Beck, S., & Trowsdale, J. (2003). The human TREM gene cluster at 6p21.1 encodes both activating and inhibitory single IgV domain receptors and includes NKp44. *European Journal of Immunology*, *33*(2), 567–577. https://doi.org/10.1002/immu.200310033

Atagi, Y., Liu, C.-C., Painter, M. M., Chen, X.-F., Verbeeck, C., Zheng, H., ... Bu, G. (2015). Apolipoprotein E is a ligand for triggering receptor expressed on myeloid cells 2 (TREM2). *Journal of Biological Chemistry*, *290*(43), 26043–26050. https://doi.org/10.1074/jbc.M115.679043

Barlowe, C., & Helenius, A. (2016). Cargo capture and bulk flow in the early secretory pathway. *Annual Review of Cell and Developmental Biology*, *32*(1), 197–222. https://doi.org/10.1146/annurev-cellbio-111315-125016

Cheng, Q., Danao, J., Talreja, S., Wen, P., Yin, J., Sun, N., ... Sambashivan, S. (2018). TREM2-activating antibodies abrogate the negative pleiotropic effects of the Alzheimer's disease variant Trem2 R47H on murine myeloid cell function. *Journal of Biological Chemistry*, *293*(32), 12620–12633. https://doi.org/10.1074/jbc.RA118.001848

Colonna, M. (2003a). DAP12 signaling: From immune cells to bone modeling and brain myelination. *Journal of Clinical Investigation*, *111*(3), 313–314. https://doi.org/10.1172/JCI200317745

Colonna, M. (2003b). TREMs in the immune system and beyond. *Nature Reviews Immunology*, *3*(6), 445–453. https://doi.org/10.1038/nri1106

Colonna, M., & Wang, Y. (2016). TREM2 variants: New keys to decipher Alzheimer disease pathogenesis. *Nature Reviews Neuroscience*, *17*(4), 201–207. https://doi.org/10.1038/nrn.2016.7

Fadok, V. A., Voelker, D. R., Campbell, P. A., Cohen, J. J., Bratton, D. L., & Henson, P. M. (1992). Exposure of phosphatidylserine on the surface of apoptotic lymphocytes triggers specific recognition and removal by macrophages. *Journal of Immunology (Baltimore, MD)*, *148*(7), 2207–2216.

Farfara, D., Trudler, D., Segev-Amzaleg, N., Galron, R., Stein, R., & Frenkel, D. (2011). γ-Secretase component presenilin is important for microglia β-amyloid clearance. *Annals of Neurology*, *69*(1), 170–180. https://doi.org/10.1002/ana.22191

Feuerbach, D., Schindler, P., Barske, C., Joller, S., Beng-Louka, E., Worringer, K. A., ... Neumann, U. (2017). ADAM17 is the main sheddase for the generation of human triggering receptor expressed in myeloid cells (hTREM2) ectodomain and cleaves TREM2 after histidine 157. *Neuroscience Letters*, *660*, 109–114. https://doi.org/10.1016/j.neulet.2017.09.034

Filipello, F., Morini, R., Corradini, I., Zerbi, V., Canzi, A., Michalski, B., ... Matteoli, M. (2018). The microglial innate immune receptor TREM2 is required for synapse elimination and Normal brain connectivity. *Immunity*, *48*, 979–991. https://doi.org/10.1016/j.immuni.2018.04.016

Frank, S., Burbach, G. J., Bonin, M., Walter, M., Streit, W., Bechmann, I., & Deller, T. (2008). TREM2 is upregulated in amyloid plaque-associated microglia in aged APP23 transgenic mice. *Glia*, *56*(13), 1438–1447. https://doi.org/10.1002/glia.20710

Glebov, K., Wunderlich, P., Karaca, I., & Walter, J. (2016). Functional involvement of γ-secretase in signaling of the triggering receptor expressed on myeloid cells-2 (TREM2). *Journal of Neuroinflammation*, *13*(1), 17. https://doi.org/10.1186/s12974-016-0479-9

Guerreiro, R., Wojtas, A., Bras, J., Carrasquillo, M., Rogaeva, E., Majounie, E., ... Hardy, J. (2013). TREM2 variants in Alzheimer's Disease. *New England Journal of Medicine*, *368*(2), 117–127. https://doi.org/10.1056/NEJMoa1211851

Hakola, H. P. A., Järvi, O. H., & Sourander, P. (2009). Osteodysplasia polycystica hereditaria combined with sclerosing leucoencephalopathy. *Acta Neurologica Scandinavica*, *46*(S43), 79–80. https://doi.org/10.1111/j.1600-0404.1970.tb02161.x

Hammond, C., & Helenius, A. (1994). Quality control in the secretory pathway: Retention of a misfolded viral membrane glycoprotein involves cycling between the ER, intermediate compartment, and golgi apparatus. *The Journal of Cell Biology*, *126*(1), 41–52. https://doi.org/10.1083/jcb.126.1.41

Hsieh, C. L., Koike, M., Spusta, S. C., Niemi, E. C., Yenari, M., Nakamura, M. C., & Seaman, W. E. (2009). A role for TREM2 ligands in the phagocytosis of apoptotic neuronal cells by microglia. *Journal of Neurochemistry*, *109*(4), 1144–1156. https://doi.org/10.1111/j.1471-4159.2009.06042.x

Humphrey, M. B., Xing, J., & Titus, A. (2015). The TREM2-DAP12 signaling pathway in Nasu-Hakola disease: A molecular genetics perspective. *Research and Reports in Biochemistry*, *5*, 89. https://doi.org/10.2147/RRBC.S58057

Jay, T. R., Saucken, V. E., Muñoz, B., Codocedo, J. F., Atwood, B. K., Lamb, B. T., & Landreth, G. E. (2019). TREM2 is required for microglial instruction of astrocytic synaptic engulfment in neurodevelopment. *Glia*, *67*(10), glia.23664. https://doi.org/10.1002/glia.23664

Jay, T. R., von Saucken, V. E., & Landreth, G. E. (2017). TREM2 in neurodegenerative diseases. *Molecular Neurodegeneration*, *12*(1), 56. https://doi.org/10.1186/s13024-017-0197-5

Jonsson, T., Stefansson, H., Steinberg, S., Jonsdottir, I., Jonsson, P. V., Snaedal, J., ... Stefansson, K. (2013). Variant of TREM2 associated with the risk of Alzheimer's Disease. *New England Journal of Medicine*, *368*(2), 107–116. https://doi.org/10.1056/NEJMoa1211103

Kaneko, M., Sano, K., Nakayama, J., & Amano, N. (2010). Nasu-Hakola disease: The first case reported by Nasu and review: The 50th anniversary of Japanese Society of Neuropathology. *Neuropathology: Official Journal of the Japanese Society of Neuropathology*, *30*(5), 463–470. https://doi.org/10.1111/j.1440-1789.2010.01127.x

Karsak, M., Glebov, K., Scheffold, M., Bajaj, T., Kawalia, A., Karaca, I., ... Ramirez, A. (2020). A rare heterozygous TREM2 coding variant identified in familial clustering of dementia affects an intrinsically disordered protein region and function of TREM2. *Human Mutation*, *41*(1), 169–181. https://doi.org/10.1002/humu.23904

Kemmerling, N., Wunderlich, P., Theil, S., Linnartz-Gerlach, B., Hersch, N., Hoffmann, B., ... Walter, J. (2017). Intramembranous processing by γ-secretase regulates reverse signaling of ephrin-B2 in migration of microglia. *Glia*, *65*(7), 1103–1118. https://doi.org/10.1002/glia.23147

Kleinberger, G., Yamanishi, Y., Suarez-Calvet, M., Czirr, E., Lohmann, E., Cuyvers, E., ... Haass, C. (2014). TREM2 mutations implicated in neurodegeneration impair cell surface transport and phagocytosis. *Science Translational Medicine*, *6*(243), 243ra86. https://doi.org/10.1126/scitranslmed.3009093

Klesney-Tait, J., Turnbull, I. R., & Colonna, M. (2006). The TREM receptor family and signal integration. *Nature Immunology*, *7*(12), 1266–1273. https://doi.org/10.1038/ni1411

Kober, D. L., Alexander-Brett, J. M., Karch, C. M., Cruchaga, C., Colonna, M., Holtzman, M. J., & Brett, T. J. (2016). Neurodegenerative disease mutations in TREM2 reveal a functional surface and distinct loss-of-function mechanisms. *eLife*, *5*, 1–24. https://doi.org/10.7554/eLife.20391

Le Ber, I., De Septenville, A., Guerreiro, R., Bras, J., Camuzat, A., Caroppo, P., ... Brice, A. (2014). Homozygous TREM2 mutation in a family with atypical frontotemporal dementia. *Neurobiology of Aging*, *35*(10), 2419.e23–2419.e25. https://doi.org/10.1016/j.neurobiolaging.2014.04.010

Leslie, R. G. Q., Melamed, M. D., & Cohen, S. (1971). The products from papain and pepsin hydrolyses of Guinea-pig immunoglobulins γ1G and γ2G. *Biochemical Journal*, *121*(5), 829–837. https://doi.org/10.1042/bj1210829

Nadler, Y., Alexandrovich, A., Grigoriadis, N., Hartmann, T., Rao, K. S. J., Shohami, E., & Stein, R. (2008). Increased expression of the γ-secretase components presenilin-1 and nicastrin in activated astrocytes and microglia following traumatic brain injury. *Glia*, *56*(5), 552–567. https://doi.org/10.1002/glia.20638

Nasu, T., Tsukahara, Y., & Terayama, K. (1973). A lipid metabolic disease—"Membraneous lipodystrophy"—an autopsy case demonstrating numerous peculiar membrane-structures composed of compound lipid in bone and bone marrow and various adipose tissues. *Pathology International*, *23*(3), 539–558.

Paloneva, J., Mandelin, J., Kiialainen, A., Böhling, T., Prudlo, J., Hakola, P., ... Peltonen, L. (2003). DAP12/TREM2 deficiency results in impaired osteoclast differentiation and osteoporotic features. *Journal of Experimental Medicine*, *198*(4), 669–675. https://doi.org/10.1084/jem.20030027

Paloneva, J., Manninen, T., Christman, G., Hovanes, K., Mandelin, J., Adolfsson, R., ... Peltonen, L. (2002). Mutations in two genes encoding different subunits of a receptor signaling complex result in an identical disease phenotype. *American Journal of Human Genetics*, *71*(3), 656–662. https://doi.org/10.1086/342259

Park, J.-S., Ji, I. J., An, H. J., Kang, M.-J., Kang, S.-W., Kim, D.-H., & Yoon, S.-Y. (2015). Disease-associated mutations of TREM2 alter the processing of N-linked oligosaccharides in the Golgi apparatus. *Traffic*, *16*(5), 510–518. https://doi.org/10.1111/tra.12264

Prada, I., Ongania, G. N., Buonsanti, C., Panina-Bordignon, P., & Meldolesi, J. (2006). Triggering receptor expressed in myeloid cells 2 (TREM2)

trafficking in microglial cells: Continuous shuttling to and from the plasma membrane regulated by cell stimulation. *Neuroscience*, *140*(4), 1139–1148. https://doi.org/10.1016/j.neuroscience.2006.03.058

Price, B. R., Sudduth, T. L., Weekman, E. M., Johnson, S., Hawthorne, D., Woolums, A., & Wilcock, D. M. (2020). Therapeutic Trem2 activation ameliorates amyloid-beta deposition and improves cognition in the 5XFAD model of amyloid deposition. *Journal of Neuroinflammation*, *17*(1), 238. https://doi.org/10.1186/s12974-020-01915-0

Satoh, J. I., Tabunoki, H., Ishida, T., Yagishita, S., Jinnai, K., Futamura, N., … Arima, K. (2011). Immunohistochemical characterization of microglia in Nasu-Hakola disease brains. *Neuropathology*, *31*(4), 363–375. https://doi.org/10.1111/j.1440-1789.2010.01174.x

Schlepckow, K., Kleinberger, G., Fukumori, A., Feederle, R., Lichtenthaler, S. F., Steiner, H., & Haass, C. (2017). An Alzheimer-associated TREM2 variant occurs at the ADAM cleavage site and affects shedding and phagocytic function. *EMBO Molecular Medicine*, *9*(10), 1356–1365. https://doi.org/10.15252/emmm.201707672

Schlepckow, K., Monroe, K. M., Kleinberger, G., Cantuti-Castelvetri, L., Parhizkar, S., Xia, D., … Haass, C. (2020). Enhancing protective microglial activities with a dual function TREM2 antibody to the stalk region. *EMBO Molecular Medicine*, *12*(4), e11227. https://doi.org/10.15252/emmm.201911227

Sirkis, D. W., Aparicio, R. E., & Schekman, R. (2017). Neurodegeneration-associated mutant TREM2 proteins abortively cycle between the ER and ER–Golgi intermediate compartment. *Molecular Biology of the Cell*, *28*(20), 2723–2733. https://doi.org/10.1091/mbc.e17-06-0423

Song, W. M., Joshita, S., Zhou, Y., Ulland, T. K., Gilfillan, S., & Colonna, M. (2018). Humanized TREM2 mice reveal microglia-intrinsic and -extrinsic effects of R47H polymorphism. *The Journal of Experimental Medicine*, *215*(3), 745–760. https://doi.org/10.1084/jem.20171529

Sudom, A., Talreja, S., Danao, J., Bragg, E., Kegel, R., Min, X., … Wang, Z. (2018). Molecular basis for the loss-of-function effects of the Alzheimer's disease-associated R47H variant of the immune receptor TREM2. *Journal of Biological Chemistry*, *293*(32), 12634–12646. https://doi.org/10.1074/jbc.RA118.00235

Thornton, P., Sevalle, J., Deery, M. J., Fraser, G., Zhou, Y., Ståhl, S., … Crowther, D. C. (2017). TREM2 shedding by cleavage at the H157-S158 bond is accelerated for the Alzheimer's disease-associated H157Y variant. *EMBO Molecular Medicine*, *9*(10), 1366–1378. https://doi.org/10.15252/emmm.201707673

Walter, J. (2016). The triggering receptor expressed on myeloid cells 2: A molecular link of Neuroinflammation and neurodegenerative diseases. *Journal of Biological Chemistry*, *291*(9), 4334–4341. https://doi.org/10.1074/jbc.R115.704981

Walter, J., Kemmerling, N., Wunderlich, P., & Glebov, K. (2017). γ-Secretase in microglia - implications for neurodegeneration and neuroinflammation. *Journal of Neurochemistry*, *143*(4), 445–454. https://doi.org/10.1111/jnc.14224

Wang, S., Mustafa, M., Yuede, C. M., Salazar, S. V., Kong, P., Long, H., … Colonna, M. (2020). Anti-human TREM2 induces microglia proliferation and reduces pathology in an Alzheimer's disease model. *Journal of Experimental Medicine*, *217*(9), e20200785. https://doi.org/10.1084/jem.20200785.

Wang, Y., Cella, M., Mallinson, K., Ulrich, J. D., Young, K. L., Robinette, M. L., … Colonna, M. (2015). TREM2 lipid sensing sustains the microglial response in an Alzheimer's Disease model. *Cell*, *160*(6), 1061–1071. https://doi.org/10.1016/j.cell.2015.01.049

Wes, P. D., Sayed, F. A., Bard, F., & Gan, L. (2016). Targeting microglia for the treatment of Alzheimer's Disease. *Glia*, *64*(10), 1710–1732. https://doi.org/10.1002/glia.22988

Wunderlich, P., Glebov, K., Kemmerling, N., Tien, N. T., Neumann, H., & Walter, J. (2013). Sequential proteolytic processing of the triggering receptor expressed on myeloid cells-2 (TREM2) protein by ectodomain shedding and γ-secretase-dependent intramembranous cleavage. *Journal of Biological Chemistry*, *288*(46), 33027–33036. https://doi.org/10.1074/jbc.M113.517540

Yao, H., Coppola, K., Schweig, J. E., Crawford, F., Mullan, M., & Paris, D. (2019). Distinct signaling pathways regulate TREM2 phagocytic and NFκB antagonistic activities. *Frontiers in Cellular Neuroscience*, *13*, 457. https://doi.org/10.3389/fncel.2019.00457

Yeh, F. L., Wang, Y., Tom, I., Gonzalez, L. C., & Sheng, M. (2016). TREM2 binds to apolipoproteins, including APOE and CLU/APOJ, and thereby facilitates uptake of amyloid-Beta by microglia. *Neuron*, *91*(2), 328–340. https://doi.org/10.1016/j.neuron.2016.06.015

Zhao, Y., Li, X., Huang, T., Jiang, L., Tan, Z., Zhang, M., … Xu, H. (2017). Intracellular trafficking of TREM2 is regulated by presenilin 1. *Experimental & Molecular Medicine*, *49*(12), e405–e405. https://doi.org/10.1038/emm.2017.200

Zhao, Y., Wu, X., Li, X., Jiang, L.-L., Gui, X., Liu, Y., … Xu, H. (2018). TREM2 is a receptor for β-amyloid that mediates microglial function. *Neuron*, *97*(5), 1023–1031.e7. https://doi.org/10.1016/j.neuron.2018.01.031

Zhong, L., Chen, X.-F., Wang, T., Wang, Z., Liao, C., Wang, Z., … Bu, G. (2017). Soluble TREM2 induces inflammatory responses and enhances microglial survival. *Journal of Experimental Medicine*, *214*(3), 597–607. https://doi.org/10.1084/jem.20160844

Zhong, L., Chen, X.-F., Zhang, Z.-L., Wang, Z., Shi, X.-Z., Xu, K., … Bu, G. (2015). DAP12 stabilizes the C-terminal fragment of the triggering receptor expressed on myeloid Cells-2 (TREM2) and protects against LPS-induced pro-inflammatory response. *Journal of Biological Chemistry*, *290*(25), 15866–15877. https://doi.org/10.1074/jbc.M115.645986

Zhong, L., Wang, Z., Wang, D., Wang, Z., Martens, Y. A., Wu, L., … Chen, X.-F. (2018). Amyloid-beta modulates microglial responses by binding to the triggering receptor expressed on myeloid cells 2 (TREM2). *Molecular Neurodegeneration*, *13*(1), 15. https://doi.org/10.1186/s13024-018-0247-7

Zhong, L., Xu, Y., Zhuo, R., Wang, T., Wang, K., Huang, R., … Chen, X.-F. (2019). Soluble TREM2 ameliorates pathological phenotypes by modulating microglial functions in an Alzheimer's disease model. *Nature Communications*, *10*(1), 1365. https://doi.org/10.1038/s41467-019-09118-9